ANALYTICAL SCIENCES OCTOBER 2008, VOL. 24

RAIRS Investigations on Films of the Ionic Liquid [EMIM]Tf_2N

Oliver HÖFFT,* Stephan BAHR,*, and Volker KEMPTER*†**

**Technische Universität Clausthal, Institut für Physik und Physikalische Technologien, Leibnizstr. 4, D-38678 Clausthal-Zellerfeld, Germany*
***Universität Osnabrück, Fachbereich Physik, Barbarastrasse 7, D-49076 Osnabrück, Germany*

The reflection-absorption infrared (RAIRS) spectra of 1-ethyl-3-methylimidazolium bis(trifluoromethylsulfonyl)imide ([EMIM]Tf_2N) are presented for liquid as well as for amorphous and crystalline solid films. The liquid and amorphous films show rather similar spectra, indicating that the film structure is similar in both cases. On the other hand, these spectra differ considerably from those of crystalline films, indicating that the film structure is different for liquid and crystalline films. There are however indications that in all of the studied phases, including the crystalline state, the cation interaction with the SO_2 groups of the anion dominates.

(Received April 18, 2008; Accepted June 4, 2008; Published October 10, 2008)

Introduction

Room-temperature ionic liquids (RT-ILs) have attracted much attention owing to their excellent properties, the most obvious ones being their wide temperature range of liquid phase, very low vapor pressure at RT, chemical stability, their potential as "green" solvents,[1,2] and their high heat capacities. These properties make them good candidates for use in many fields,[2,3] such as thermal storage,[4] electrochemical applications,[5] homogeneous catalysis[2,6,7] and dye-sensitized solar cells.[8] Moreover, 1-ethyl-3-methylimidazolium bis(trifluoromethylsulfonyl)imide ([EMIM]Tf_2N) is member of a class of ILs that can apparently be distilled at reduced pressure at moderate temperatures.[9,10] Important applications of ILs require knowledge of their surface properties. This includes *e.g.* new electrolytes for electrodeposition,[11] and electrochemical devices, such as Li ion batteries[12] and fuel cells.[13] The potential application of ionic liquid films for submicron-resolution lithographic imaging[14] and for the construction of a Lunar Liquid Mirror[15] should also be mentioned here.

In order to be able to refine the performance of RT-ILs, detailed knowledge of the geometric, electronic and vibrational structure of RT-ILs, also particularly in surface region (up to a depth of about 1 nm below the surface), appears to be indispensable in the temperature regime between 100 and 700 K.

In previous work we have applied metastable impact electron spectroscopy (MIES), in combination with various photoelectron spectroscopies (X-ray photoelectron spectroscopy (XPS), ultraviolet photoelectron spectroscopy (UPS) with HeI and II radiation), to study the electronic structure of a typical RT-IL, [EMIM]Tf_2N (see inset in Figs. 1 and 2), deposited on a polycrystalline Au substrate.[16] MIES is ultimately surface sensitive (zero depth information).[17,18] By combining MIES with UPS and XPS, covering a wide range of depth resolution (from zero to about 5 nm below the surface), we obtained not only information on the termination of the RT-IL film, but also on its surface-near region. The results were later interpreted by us on the basis of DFT calculations on isolated ion pairs.[19,20] While these studies delivered considerable insight into the structure of the surface-near region at room temperature (RT), the change in the structure of the films during the liquid-to-amorphous solid phase transition, which takes place during fast cooling, remained poorly understood.

In order to obtain additional information on the eventual differences in the bonding properties in the liquid and solid (amorphous and crystalline) states, we applied reflection-absorption infrared spectroscopy (RAIRS) to liquid and solid films of [EMIM]Tf_2N. IR measurements on bulk liquid [EMIM]Tf_2N, carried out at RT, are available for comparison (see below). Support for the interpretation of the results can be expected from the recent Density-Functional Theory (DFT) and Molecular-Dynamic (MD) calculations, carried out on [EMIM]Tf_2N clusters[21] and the bulk liquid.[22,23]

Experimental

The ultrahigh vacuum (UHV) system (base pressure 5×10^{-10} mbar) employed for the present studies was equipped with MIES, UPS (HeI and II) and XPS, allowing for cross referencing with earlier data on [EMIM]Tf_2N, and RAIRS. A polycrystalline Ag sample served as support for the IL film. [EMIM]Tf_2N (Merck/EMD) was purchased in high-purity quality. For purification, the ionic liquid was dried under vacuum and stirring conditions for 12 h at a temperature of 80°C to a water content below 3 ppm (by Karl–Fischer titration). The samples were prepared by spin-coating the Ag substrate with one droplet of the RT-IL, and were, after outgassing carefully, introduced into the UHV chamber. Naked-eye control gave several microns as a rough estimate for the film thickness; at any rate, XPS provided a lower limit of 10 nm for the film thickness. The [EMIM]Tf_2N samples prepared in this way had very low vapor pressure, and no change of the UHV chambers base pressure could be detected during measurements performed at

† To whom correspondence should be addressed.
E-mail: v.kempter@pe.tu-clausthal.de

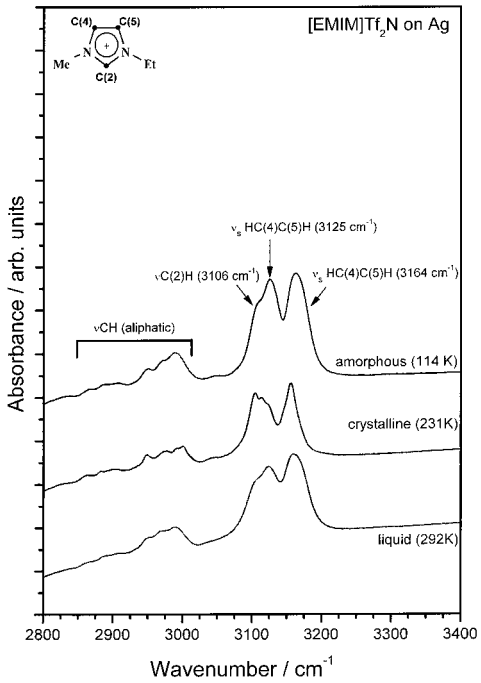

Fig. 1 RAIRS spectra collected between 2850 and 3200 cm^{-1} during heating (114 to 292 K) of an amorphous [EMIM]Tf_2N film on Ag.

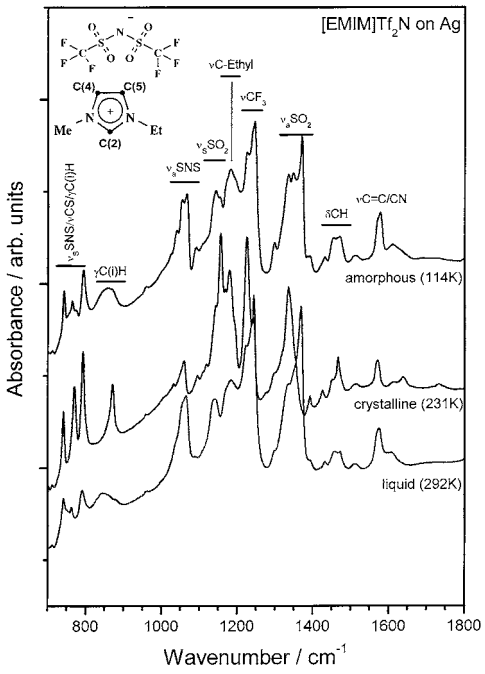

Fig. 2 RAIRS spectra collected between 800 and 1600 cm^{-1} during heating (114 to 292 K) of an amorphous [EMIM]Tf_2N film on Ag.

RT. The Ag sample could be cooled to 114 K using liquid-nitrogen cooling facilities, and the sample temperature could be measured with a thermocouple in direct contact with the front of the Ag target. It was verified by MIES and UPS that, as far as the electronic structure of the films prepared on Ag is concerned, their properties are identical with those prepared by similar procedures on Au.[16,19,20]

The RAIRS setup contained a Bruker IFS 66v/S vacuum Fourier transform infrared spectrometer, connected directly to a UHV chamber. The Mid-IR beam was coupled to the UHV system through KBr optics, and focussed under an angle of 83.5 degs to the surface normal onto the silver substrate. The MCT (mercury-cadium-telluride) detector's cut-off was at 700 cm^{-1}; thus, the region from 4000 down to 700 cm^{-1} could be used for interpretation of the vibrational spectrum of the adsorbed [EMIM]Tf_2N film. Normally, the spectra were recorded with a resolution of 4 cm^{-1}, and 270 scans were added prior to a Fourier transformation and a calculation of the absorbance (as the negative logarithm of the ratio of a sample spectrum to a spectrum of the clean surface).

Results

Assignment of spectral structures

In identifying of the spectral features, seen in the range between 2850 and 3200 cm^{-1} (Fig. 1), we were guided by the Fourier transform infrared spectroscopy (FTIR) and Raman results on liquid [EMIM]Tf_2N.[21,24-29] Accordingly, the aliphatic C–H modes of the CH_2 group, the CH_3 terminal group of the ethyl chain, and the CH_3 group bonded to the [EMIM] ring are seen between 2850 and about 3000 cm^{-1}. The spectrum, in its general structure, resembles that for [BMIM]BF_4, discussed in some detail in Ref. 29 although the structure of the two groups centred around 2900 and 2980 cm^{-1} appears to be slightly more complicated in the present case.

The structure, seen between about 3080 and 3200 cm^{-1}, is attributed to the C–H stretching modes involving the C-atoms of the [EMIM] ring. We assign the peaks at 3125 (3164) cm^{-1} to the antisymmetric (symmetric) stretching modes of HC(4)–C(5)H (in the following denoted as ν_aHC(4)C(5)H and ν_sHC(4)C(5)H, respectively) and the shoulder seen around 3106 cm^{-1} to the C(2)–H stretching mode, subsequently denoted as νC(2)H.[24,26,28] All features are seen in both the spectra from the liquid (amorphous) and crystalline states, although with different relative intensities.

The assignment of the various groups of spectral features seen between 800 and 1600 cm^{-1}, *i.e.* the coarse structure in that spectral regime (see as bars in Fig. 2), was made on the basis of the available literature, in particular Refs. 30 and 31 for Tf_2N, and Refs. 25, 32 – 34 for EMIM. In particular, strong activity is due to the modes ν_sSNS/ν_sCS (720 to 800 cm^{-1}), ν_aSNS (1010 to 1080 cm^{-1}), νC-ethyl (methyl) (1160 to 1200 cm^{-1}), $\nu_a CF_3$ (1200 to 1240 cm^{-1}), $\nu_a SO_2$ (1300 to 1400 cm^{-1}) and νC=C/νCN (1420 to 1490 cm^{-1}). The symbols have the usual meaning: ν, stretching; δ, bending; γ, out-of-plane; s, symmetric; a, antisymmetric. Again, all of the mentioned features are seen both in the spectra from the liquid (amorphous) and crystalline states, although with different relative intensities. On the other hand, a full understanding of the fine structure of the various bands requires further research.

Because $\nu_a SO_2$ (1300 to 1400 cm^{-1}) is well-separated from any other bands, the changes of its shape and intensity as a function of the phase, liquid, amorphous and crystalline, of the film are discussed in more detail below.

Comparison with literature spectra

In Fig. 3 we present a comparison of our spectra for liquid and crystalline films of [EMIM]Tf_2N on Ag with those from the corresponding bulk liquid[35] (see also Ref. 30). While the general structure appears to be the same in all displayed spectra, there are significant differences in the shape of the $\nu_a CF_3$ and $\nu_a SO_2$ stretching bands. Even though most of the fine structure,

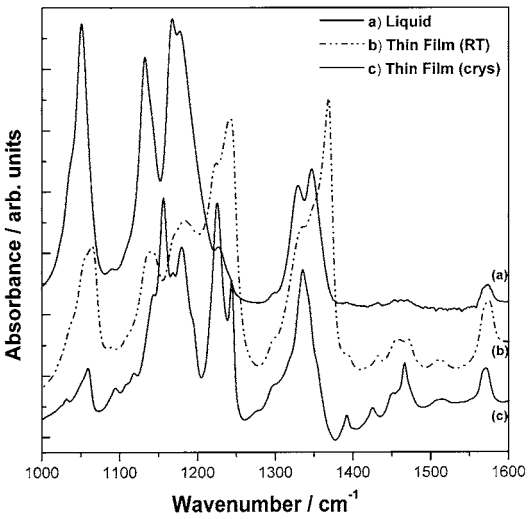

Fig. 3 [EMIM]Tf_2N infrared spectra from the bulk liquid (Ref. 35) (a), liquid films on Ag (present work) (b) and from crystalline films on Ag (present work) (c).

seen for the bulk liquid, is also visible in the spectra of the films prepared on Ag, the relative contribution of the various fine-structure components is different for the films, particularly for the CF_3 and SO_2 stretching bands. On the other hand, the EMIM-related absorption bands, particularly those originating from the ring stretching (around 1570 cm^{-1}), and the CH_3 bending modes (around 1450 cm^{-1}) are rather similar for the films on Ag and for the bulk liquid. We conclude that substrate effects are responsible for the differences observed in the spectra from the bulk and the films. Substrate effects can originate as follows: under the studied conditions the first liquid layer, adsorbed on the Ag, could be composed preferentially of either cations or anions. One possible reason for the latter type of preferential adsorption could be the soft base character of the N atom. As a consequence, the preferential adsorption in the first layer could affect the growth of additional layers, leading to local structures that are different from those found in the bulk liquid. Such local structures manifest themselves most clearly in the bands that originate from groups that are directly involved in the cation-anion interaction, not so much in bands that involve the ring skeleton. Although RAIRS spectra for the crystalline state, to our knowledge, were not reported so far, it is likely that a preferential adsorption would affect the crystalline growth as well.

Phase dependence of the film spectra

As far as the cation-related activity in the considered spectral range is concerned, we concentrate on the C–H stretching modes of the [EMIM] ring (3100 to 3200 cm^{-1}). For the anion-related intensity we concentrate on that of the strong bands between about 1200 and 1400 cm^{-1}, assigned to the antisymmetric stretching modes ν_aCF_3 and ν_aSO_2 of the CF_3 and SO_2 groups, respectively; these bands show the most pronounced dependence on the phase of the film, and, moreover, the CF_3 and SO_2 groups are directly involved in the cation-anion interaction, at least in the crystalline state.[36] Thus, they can be expected to supply detailed information on eventual changes of the cation-anion bonding properties during the liquid-to-solid phase transition.

Differential scanning calorimetry (DSC)[36] and TOF-SIMS[37] have shown that, at cooling rates faster than 0.2 K s^{-1}, a transition from the liquid state into a glassy state takes place whereby small changes are only observed in the SIMS spectra.[37] Thus, the amorphous state of [EMIM]Tf_2N can be obtained directly from the liquid state when employing a moderate cooling speed. On the other hand, it has been demonstrated that at sufficiently slow cooling rates a liquid-to-crystalline transition takes place upon cooling.[37] It has been established by DSC[36] and SIMS[37] (and confirmed in this work) that the crystallization of an amorphous film sets in when the temperature (heating rate 0.5 K s^{-1}) approaches the glass transition temperature of 227 K. It is also known from DSC[36] and SIMS[37] (and from this work) that, when increasing the temperature further, the crystalline film starts to melt at around 260 K.

Figures 1 and 2 compare the spectra obtained from a liquid film held at 292 K, an amorphous film, produced by fast cooling the liquid film (cooling rate 0.5 K s^{-1}) from 292 to 114 K, and from a crystalline film, produced by heating the amorphous film from 114 to 231 K. Only small changes are seen in the RAIRS spectra during the liquid-to-amorphous transition (compare the top and bottom spectra). According to Ref. 38, the structures present in the liquid film are preserved upon cooling, *i.e.* the ionic species present in the liquid film have insufficient time to reorganize in the form of a crystalline film at the used cooling rate. This implies also that the bonding properties, found in the liquid film, remain essentially the same upon cooling to an amorphous phase, explaining the comparatively small changes observed in the corresponding RAIRS spectra. On the basis of what is known from DSC and TOF-SIMS, we attribute the drastic changes seen in the RAIRS spectra around at 227 K to an amorphous-to-crystalline transition, and those at around 260 K to the crystalline-to-liquid transition. During this melting process, the spectral structure characteristic of the amorphous state are largely recovered, both as far as the C–H stretching modes, involving the C-atoms of the [EMIM] ring, and the anion-induced structures, ν_aCF_3 and ν_aSO_2, in particular, are concerned.

For a more quantitative analysis of the bands resulting from the C–H stretching modes of the [EMIM] ring, we have, as demonstrated successfully in Ref. 28, decomposed them into 3 Gaussian-shaped peaks, representing the three stretching modes introduced above. This analysis shows that, as a result of crystallization, the intensity of both $\nu_aHC(4)C(5)H$ and $\nu_sHC(4)C(5)H$ decreases by a factor of two, while the intensity of $\nu C(2)H$ remains practically constant. For both ν_aCF_3 and ν_aSO_2 the sharp peaks, forming the high wavelength cutoffs of the respective bands, disappear as a consequence of the crystallization; the center of both bands shifts towards lower wavenumbers.

Discussion

In the following, a model is discussed that allows to visualize our main findings taking place during the amorphous-to-crystalline and crystalline-to-liquid transitions, namely the drop of the intensity of the HC(4)C(5)H stretching modes (whereas that of the C(2)–H stretch remains constant), and the characteristic changes taking place in the bands representing the SO_2 and CF_3 stretching modes. For the following considerations we rely on the recent theory results of Refs. 22 and 23; in these studies the static distributions (radial and spatial distributions) of the anions and cations around a chosen cation were calculated with the help of classical MD calculations.

The following findings are of particular importance for the present work: (1) The cation-anion interaction in the liquid phase is mainly between the C(2)–H group of the [EMIM] ring

and the O atom of the SO_2 group of the Tf_2N anion. (2) Linear complexes of the type C–H···O do not dominate the interaction;[22,23] instead, the O-atoms are found preferentially above and underneath the [EMIM] ring, although in the neighborhood of the C(2)–H groups. Based on our results, *i.e.* the similarity of the RAIRS spectra in the liquid and amorphous solid states, we anticipate that in the amorphous phase the interaction mechanism is the same as in the liquid phase, *i.e.* in both situations the interaction is characterized by (1) and (2). In the crystalline state the Tf_2N anions do also interact with the C(2)–H group of [EMIM] ring, again *via* the O-atoms of the SO_2 groups. However, other than in the liquid, linear complexes of the type C–H···O are formed that can be described as moderately strong "standard" H-bonds.[36] Moreover, also in the crystalline state, the C(4)H and C(5)H groups are involved in the formation of the crystalline network, again *via* H-bonds involving the SO_2 groups. The resulting layers of the H-bonded network are linked to each other *via* the CF_3 groups.

In order to explain our results, our argumentation is as follows: in the liquid state, the interaction of the C(2)H groups with the SO_2 groups of the anion leads to the observed, considerable reduction of the intensity of νC(2)H as compared to ν_aHC(4)C(5)H and ν_sHC(4)C(5)H (which originate from the non-interacting C(4)H and C(5)H groups). Obviously, not all of the CF_3 and SO_2 groups of the anion interact with cations. These non-interacting groups give rise to the sharp peaks in the bands of the CF_3 and SO_2 stretching modes around 1240 and 1340 cm^{-1}, respectively. These peaks are located close to the positions where the corresponding bands would be expected for isolated CF_3 and SO_2 groups. In the crystalline state, in addition to the C(2)H groups, also all C(4)H and C(5)H groups become involved into the interaction with anions (again *via* SO_2 groups) because of the formation of the H-bonded network (see above). Moreover, also all CF_3 groups contribute to the (interlayer) stabilization of the network. The involvement of all C(4)H and C(5)H groups into the cation-anion interaction (*via* the SO_2 groups) as well as the involvement of the CF_3 groups in the bonding has the following consequences:

(1) The intensity of the ν_aHC(4)C(5)H and ν_sHC(4)C(5)H bands decreases by the observed factor of two, and becomes comparable with the intensity of νC(2)H. This appears to be plausible because the environment experienced by the C(*i*)–H groups in the crystalline structure is similar for i = 2, 4 and 5.

(2) All of SO_2 groups become integrated into the cation-anion interaction (*via* the formation of H-bonds with the C(*i*)H groups). Thus, the sharp peak at the high-wavenumber cutoff of the $\nu_a SO_2$ band noticed in the liquid state (attributed to the presence of SO_2 groups not involved into the interaction with cations), disappears, and the center of the corresponding band moves to lower wavenumbers (around 1340 cm^{-1}), as expected for bonded SO_2 species.

(3) Also, all CF_3 groups are now involved into the interaction with cations because they are responsible for the interlayer stabilization of the crystalline network.[36] Consequently, for the same reason as discussed for the $\nu_a SO_2$ band, the sharp peak at the high-wavenumber cutoff disappears, being replaced by a pronounced feature at lower wavenumbers (around 1200 cm^{-1}).

During melting, *i.e.* when heating the film beyond about 260 K, the H-bonded crystalline network is destroyed, and, according to the similarity of the RAIRS spectra for the amorphous and the liquid states, the structures present in the amorphous state are recovered to a large extent.

Summarizing this section, given the correctness of the model introduced above, our results suggest: (a) The interaction is substantially different in the crystalline and liquid (amorphous) states. Only in the crystalline phase are linear complexes of the type C–H···O–SO formed while otherwise the SO_2 groups are located above and below the EMIM ring, although close to the C(2)H group of the rings. (b) While moderately strong H-bonds are known to exist in the crystalline state,[36] the properties of the bonds existing in the liquid (amorphous) state appear to differ considerably from those of a conventional C–H···O–SO type H-bond.

Conclusions

The reflection-absorption infrared (RAIRS) spectra of liquid and solid (amorphous and crystalline) [EMIM]Tf_2N films were collected. Amorphous films were produced by the quenching of a liquid film (deposited on Ag at 292 K) to 114 K under ultrahigh vacuum conditions. Crystalline films are obtained from amorphous ones by heating; the glass transition temperature, at which the amorphous-to-crystalline transition takes place, is about 227 K. Melting of the crystalline structure occurs around 260 K. The bands from the CH stretching modes of the [EMIM] ring and those from the CF_3 and SO_2 stretching modes were analyzed in detail. Liquid and amorphous films show rather similar spectra, suggesting that their film structure is similar. Marked differences are noticed in the spectra for the liquid, as compared to the crystalline state: the shape of the C–H bands of the [EMIM] ring and of the CF_3 and SO_2 stretching bands of the anion is characteristically different in the liquid and crystalline state. This suggests that the dominant mechanism for cation-anion interaction in liquid or amorphous solid films is different from that in crystalline films. On the one hand, there are however indications, that in both the liquid and the crystalline phase the cation-anion interaction is mainly between the CH-groups of the [EMIM] ring and the SO_2 groups of the anions. On the other hand, the complexes formed between the SO_2 groups of the anion and the CH groups at the [EMIM] ring appear to be different in the liquid (amorphous) and crystalline states (C–H···O–SO linear H-bonds in the crystalline phase, as compared to SO_2 groups located above and below the EMIM ring in the liquid phase).

Acknowledgements

We are grateful to F. Endres (Clausthal University of Technology) for supplying the [EMIM]Tf_2N sample as well as for his continuous interest in this work. O. H. acknowledges the DFG-SPP 1191 priority program Ionic Liquids for funding. We thank S. Ishiguro (Kyushu University) for providing us with the IR spectrum for bulk liquid [EMIM]Tf_2N presented in Fig. 3. Stimulating discussions of various aspects of this work with J. Günster (Oerlikon Company) and S. Krischok (TU Ilmenau) are also acknowledged.

References

1. D. Yoshimura, T. Yokoyama, T. Nishi, H. Ishii, R. Ozawa, H. Hamaguchi, and K. Seki, *J. Electron Spectrosc. Relat. Phenom.*, **2005**, *144 – 147*, 319.
2. P. Wasserscheid and W. Keim, *Angew. Chem.*, **2000**, *112*, 3926.
3. K. Binnemanns, *Chem. Rev.*, **2005**, *105*, 4148.
4. J. M. Crosthwaite, M. J. Muldoon, J. K. Dixon, J. L. Anderson, and J. F. Brennecke, *J. Chem. Thermodyn.*, **2005**,

37, 559.
5. F. Endres and S. Z. E. Abedin, *Phys. Chem. Chem. Phys.*, **2006**, *8*, 2101.
6. P. Kölle and R. Dronskowski, *Inorg. Chem.*, **2004**, *43*, 2803.
7. T. Welton, *Chem. Rev.*, **1999**, *99*, 2071.
8. C. Pinalla, M. G. D. Popolo, R. M. Lynden-Bell, and J. Kohanoff, *J. Phys. Chem. B*, **2005**, *109*, 17922.
9. L. P. N. Rebelo, J. N. Canongia Lopes, J. M. S. S. Esperanca, and E. Filipe, *J. Phys. Chem. B*, **2005**, *109*, 6040.
10. M. J. Earle, J. Esperanca, M. A. Gilea, J. N. Canongia Lopes, L. P. N. Rebelo, J. W. Magee, K. R. Seddon, and J. A. Widegren, *Nature*, **2006**, *439*, 831.
11. W. Freyland, C. A. Zell, S. Z. E. Abedin, and F. Endres, *Electrochim. Acta*, **2003**, *48*, 3053.
12. B. Garcia, S. Lavalee, G. Perron, C. Michot, and M. Armand, *Electrochim. Acta*, **2004**, *49*, 4583.
13. A. Noda, A. Susan, K. Kudo, S. Mitsushima, K. Hayamizu, and M. Watanabe, *J. Phys. Chem. B*, **2003**, *107*, 4024.
14. F. J. M. Rutten, H. Tadesse, and P. Licence, *Angew. Chem., Int. Ed.*, **2007**, *46*, 1.
15. E. F. Borra, O. Seddiki, R. Angel, D. Eisenstein, P. Hickson, K. R. Seddon, and S. P. Worden, *Nature*, **2007**, *447*, 979.
16. O. Höfft, S. Bahr, M. Himmerlich, S. Krischok, J. A. Schaefer, and V. Kempter, *Langmuir*, **2006**, *22*, 7120.
17. Y. Harada, S. Masuda, and H. Osaki, *Chem. Rev.*, **1997**, *97*, 1897.
18. H. Morgner, *Adv. At., Mol., Opt. Phys.*, **2000**, *42*, 387.
19. S. Krischok, R. Öttking, W. J. D. Beenken, M. Himmerlich, P. Lorenz, O. Höfft, S. Bahr, V. Kempter, and J. A. Schaefer, *Z. Phys. Chem.*, **2006**, *220*, 1407.
20. S. Krischok, M. Eremtchenko, M. Himmerlich, P. Lorenz, J. Uhlig, A. Neumann, R. Öttking, W. J. D. Beenken, O. Höfft, S. Bahr, V. Kempter, and J. A. Schaefer, *J. Phys. Chem. B*, **2007**, *111*, 4801.
21. T. Köddermann, C. Wertz, A. Heintz, and R. Ludwig, *ChemPhysChem*, **2006**, *7*, 1944.
22. B. Qiao, C. Krekeler, R. Berger, L. Delle Site, and C. Holm, *J. Phys. Chem. B*, **2008**, *112*, 1743.
23. K. Fujii, Y. Soejima, Y. Kyoshoin, S. Fukuda, R. Kanzaki, Y. Umebayashi, T. Yamaguchi, T. Takamuku, and S. Ishiguro, *J. Phys. Chem. B*, **2008**, *112*, 4329.
24. D. Carter and J. Pemberton, *J. Raman Spectrosc.*, **1997**, *28*, 939.
25. E. R. Talaty, S. Raja, V. J. Storhaug, A. Dölle, and W. R. Carper, *J. Phys. Chem. B*, **2004**, *108*, 13177.
26. B. D. Fitchett and J. C. Conboy, *J. Phys. Chem. B*, **2004**, *108*, 20255.
27. A. Yokozeki, D. J. Kasprzak, and M. B. Shiett, *Phys. Chem. Chem. Phys.*, **2007**, *9*, 5018.
28. Y. Jeon, J. Sung, C. Seo, H. Lim, H. Cheong, M. Kang, B. Moon, Y. Ouchi, and D. Kim, *J. Phys. Chem. B*, **2008**, *112*, 4735.
29. Y. Jeon, J. Sung, D. Kim, C. Seo, H. Cheong, Y. Ouchi, R. Ozawa, and H. Hamaguchi, *J. Phys. Chem. B*, **2008**, *112*, 923.
30. J. Kiefer, J. Fries, and A. Leipertz, *Appl. Spectrosc.*, **2007**, *61*, 1306.
31. I. Rey, P. Johansson, J. Lindgren, J. C. Lassegues, J. Grondin, and L. Servant, *J. Phys. Chem. A*, **1998**, *102*, 3249.
32. S. A. Katsyuba, P. J. Dyson, E. E. Vandyukova, A. V. Chernova, and A. Vidis, *Helv. Chim. Acta*, **2004**, *87*, 2556.
33. S. A. Katsyuba, E. E. Zvereva, A. Vidis, and P. J. Dyson, *J. Phys. Chem. A*, **2007**, *111*, 352.
34. N. E. Heimer, R. E. Del Sesto, Z. Meng, J. S. Wilkes, and W. R. Carper, *J. Mol. Phys.*, **2006**, *124*, 84.
35. K. Fujii, Y. Umebayashi, and S. Ishiguro, unpublished results, **2008**, Kyushu University, Japan.
36. A. R. Choudhury, N. Winterton, A. Steiner, A. I. Cooper, and K. A. Johnson, *CrystEngComm*, **2006**, *8*, 742745.
37. J. Günster, R. Souda, O. Höfft, and S. Krischok, *Surf. Sci.*, in press.
38. J. C. Lassègues, J. Grondin, R. Holomb, and P. Johansson, *J. Raman Spectrosc.*, **2007**, *38*, 551558.